2012

MAP1272c Encodes an NlpC/P60 Protein, an Antigen Detected in Cattle with Johne's Disease

John Bannantine
USDA-ARS, john.bannantine@usda.gov

Cari K. Lingle
University of Missouri—Kansas City

Judith R. Stabel
USDA-ARS, National Animal Disease Center, jstabel@nadc.ars.usda.gov

Kasra X. Ramyar
University of Missouri—Kansas City

Brandon L. Garcia
University of Missouri—Kansas City

See next page for additional authors

CVI
Journals.ASM.org

MAP1272c Encodes an NlpC/P60 Protein, an Antigen Detected in Cattle with Johne's Disease

John P. Bannantine,[a] Cari K. Lingle,[b] Judith R. Stabel,[a] Kasra X. Ramyar,[b] Brandon L. Garcia,[b] Alex J. Raeber,[c] Pascal Schacher,[c] Vivek Kapur,[d] and Brian V. Geisbrecht[b]

USDA-ARS-National Animal Disease Center, Ames, Iowa, USA[a]; School of Biological Sciences, University of Missouri—Kansas City, Kansas City, Missouri, USA[b]; Prionics AG, Schlieren, Switzerland[c]; and Penn State University, University Park, Pennsylvania, USA[d]

The protein encoded by MAP1272c has been shown to be an antigen of *Mycobacterium avium* subsp. *paratuberculosis* that contains an NlpC/P60 superfamily domain found in lipoproteins or integral membrane proteins. Proteins containing this domain have diverse enzymatic functions that include peptidases, amidases, and acetyltransferases. The NlpC protein was examined in comparison to over 100 recombinant proteins and showed the strongest antigenicity when analyzed with sera from cattle with Johne's disease. To further localize the immunogenicity of NlpC, recombinant proteins representing defined regions were expressed and evaluated with sera from cattle with Johne's disease. The region from amino acids 74 to 279 was shown to be the most immunogenic. This fragment was also evaluated against a commercially available enzyme-linked immunosorbent assay (ELISA). Two monoclonal antibodies were produced in mice immunized with the full-length protein, and each recognized a distinct epitope. These antibodies cross-reacted with proteins from other mycobacterial species and demonstrated variable sizes of the proteins expressed from these subspecies. Both antibodies were further analyzed, and their interaction with MAP1272c and MAP1204 was characterized by a solution-based, luminescent binding assay. These tools provide additional means to study a strong antigen of *M. avium* subsp. *paratuberculosis*.

The search for strong yet specific *Mycobacterium avium* subsp. *paratuberculosis* antigens has been a recent focus in many laboratories throughout the world (2, 17, 20, 23). This is because the bacterium is a significant veterinary pathogen of cattle, goats, and other ruminant animals. More specifically, *M. avium* subsp. *paratuberculosis* causes Johne's disease (JD), a chronic enteritis that results in weight loss due to poor absorption of nutrients through strikingly inflamed ileum and jejunum tissues (11). The dairy industry incurs substantial economic losses due to reduced milk production, premature culling, and reduced slaughter value (27). The bacterium is shed in the feces and milk of animals in the clinical phase of disease. Transmission is by ingestion of the bacterium while grazing on pastures contaminated by this shedding process. Milk, passed from the infected dam to the daughter, has also been shown as a transmission route (30).

Further driving the search for antigens is the nature of the protein preparations currently used in diagnostic tests for JD, such as the enzyme-linked immunosorbent assay (ELISA). Several types of *M. avium* subsp. *paratuberculosis* antigen preparations have been evaluated and used for serodiagnosis of JD for over 2 decades (25). These crude mycobacterial extracts or fractionated preparations naturally contain multiple proteins, lipids, and carbohydrates, most of which are highly conserved across the *Mycobacterium avium* complex (MAC). The primary focus of current research is on improving the sensitivity of the ELISA without adversely affecting the specificity. The problem of specificity has largely been overcome by incorporating an absorption step with an extract from *Mycobacterium phlei* into most ELISA protocols to remove cross-reacting antibodies (24, 38, 39). The protoplasmic antigen preparation (PPA) and lipoarabinomannan (LAM) have been adapted to commercial ELISAs (31, 38). To date, no *M. avium* subsp. *paratuberculosis* recombinant proteins have been incorporated into a commercially available ELISA for JD.

MAP1272c encodes a protein containing an NlpC/P60 superfamily domain. Similar to *Corynebacterium glutamicum* (34), there are five distinct NlpC/P60 domain-containing proteins encoded by the *M. avium* subsp. *paratuberculosis* K-10 genome sequence, including MAP0036, MAP1203, MAP1204, MAP1272c, and MAP1928c. For the purposes of this study, we have termed the MAP1272c-encoded protein NlpC. Proteins containing these domains have diverse enzymatic functions, including hydrolyases with specificity for amide linkages in peptidoglycan (1). A P60 domain-containing protein capable of peptidoglycan hydrolysis in *Listeria monocytogenes* was shown to be secreted via the SecA2-dependent mechanism (18). Mutations in *secA2* reduced the virulence of *L. monocytogenes* and *Mycobacterium tuberculosis* (8, 19, 32). *M. avium* subsp. *paratuberculosis* also has SecA2 encoded by MAP1534 (21), and deletion of this gene results in attenuation in mouse macrophages (9, 21).

We have shown previously that NlpC is antigenic; however, the thrust of that study was to apply a high-throughput recombinant protein production method (22). Therefore, its immunogenicity was not evaluated relative to that of other *M. avium* subsp. *paratuberculosis* proteins. The studies presented here evaluate the antigenicity of this protein in greater detail by comparing it to other recombinant proteins as well as a commercial ELISA. In addition, we developed monoclonal antibodies (MAbs) to this important *M. avium* subsp. *paratuberculosis* antigen for use in downstream

Received 29 March 2012 Returned for modification 23 April 2012
Accepted 11 May 2012
Published ahead of print 16 May 2012
Address correspondence to John P. Bannantine, john.bannantine@ars.usda.gov.
Supplemental material for this article may be found at http://cvi.asm.org/.

doi:10.1128/CVI.00195-12

applications and characterized their interactions with and specificities for NlpC in biochemical detail.

MATERIALS AND METHODS

Bacterial strains and culture. *M. avium* subsp. *paratuberculosis* strain K-10 was cultured in Middlebrook (MB) 7H9 broth supplemented with oleic acid, albumin, dextrose, and catalase (OADC) enrichment and mycobactin J (2 mg/liter) for 3 weeks at 37°C. *Mycobacterium avium* complex strains and other mycobacterial strains listed in Table S1 in the supplemental material were maintained in Middlebrook 7H9 broth supplemented with OADC enrichment for 4 days at 37°C. All cultures were free of contaminating organisms as assessed by absence of growth on brain heart infusion agar (BD Microbiology).

Cloning and protein production. The whole-cell sonicated extracts from mycobacterial species and isolates were prepared as previously described (35). These preparations were used as the source of antigen for this study. The full-length NlpC and all proteins spotted on the nitrocellulose array were expressed as maltose binding protein (MBP) fusion proteins and purified as described previously (5).

Both full-length and truncated versions of MAP1272c were also subcloned into the *Escherichia coli* overexpression vector pT7HMT (14). The primers for these truncated and full-length constructs are listed in Table S2 in the supplemental material. The sequence-confirmed plasmids were transformed into *E. coli* strain BL21(DE3) for overexpression and purification, which were carried out according to the general protocols outlined in reference 14. Upon completing the initial rounds of affinity purification, the polyhistidine fusion tag was proteolytically removed by adding recombinant tobacco etch virus (TEV) protease as described previously (14). The samples were then desalted into 20 mM sodium formate buffer (pH 3.5), and final purification was achieved with Resource S cation exchange chromatography using a GE Biosciences Akta fast protein liquid chromatography (FPLC) system.

NlpC truncation A (NlpC-A) was also overexpressed from a modified version of the pT7HMT vector that encodes a cysteine residue as the first amino acid of the polypeptide of interest (13). Site-specifically biotinylated Cys-NlpC-A was produced using the EZ-Link maleimide-PEG_2-biotin reagent (Thermo Fisher Scientific [Rockford, IL]) according to the manufacturer's suggestions. Successful biotinylation at this site alone (as NlpC lacks naturally occurring cysteine residues in its sequence) was confirmed by Western blotting using a streptavidin-conjugated anti-horseradish peroxidase (anti-HRP) antibody and SuperSignal Pico chemiluminescent substrate (Thermo Fisher Scientific [Rockford, IL]).

Bovine serum samples. A set of well-characterized serum samples from Prionics AG (Schlieren-Zurich, Switzerland) and the National Veterinary Services Laboratory (Ames, IA) was used to evaluate recombinant antigens by ELISA and immunoblotting. Characteristics of these serum samples are listed in Table S3 in the supplemental material.

Production of monoclonal antibodies. Monoclonal antibodies were produced using standard methods (15). Briefly, BALB/c mice were immunized three times intraperitoneally with the MAP1272c recombinant protein (100 μg per injection) suspended in 0.5 ml of phosphate-buffered saline (PBS) (pH 7.3) at 14-day intervals. The antigen was emulsified in Freund's incomplete adjuvant for all immunizations. Humoral immune responses of each mouse were evaluated by preparative immunoblot analysis using the sonicated *M. avium* subsp. *paratuberculosis* whole-cell antigen. Cell fusions with splenic lymphocytes and myeloma cells were performed on the best responder mouse. Positive antibody-secreting hybridomas were identified by immunoblot screening with culture supernatant. Stable secreting hybridomas were immunotyped using the isotype kit I from Thermo Fisher Scientific (Rockford, IL).

Purification of monoclonal antibodies 8G6 and 14C5. Mouse hybridoma cells were grown in RPMI medium supplemented with 10% fetal bovine serum and 2 mM L-glutamine. Cells were incubated at 37°C in the presence of 5% (vol/vol) CO_2. Cells were passaged upon reaching 90% confluence, which typically required 3 days of incubation time. In this manner, approximately 1 liter of conditioned culture medium was collected for each cell line and clarified by high-speed centrifugation. The samples of clarified culture medium were concentrated 10-fold and buffer exchanged by tangential-flow filtration into 20 mM borate (pH 8.3), 3.0 M NaCl, and injected onto a 5-ml HiTrap protein G-Sepharose column (GE Biosciences). Following extensive washing to remove nonspecifically bound contaminants, bound IgG was eluted from the column using a buffer of 0.1 M glycine (pH 2.0) and the eluate was immediately neutralized by adding 1/10 volume of 1 M Tris (pH 8.0). The purified IgG was concentrated and buffer exchanged into PBS for storage at 4°C until needed.

Immunoblot assay. Protein separation was conducted by electrophoresis using 12% (wt/vol) polyacrylamide gels. Electrophoretic transfer of proteins onto pure nitrocellulose was accomplished with the Bio-Rad Trans-Blot cell (Bio-Rad Laboratories, Richmond, CA) with sodium phosphate buffer (25 mM, pH 7.8) at 0.8 A for 90 min. After transfer, filters were blocked with PBS (pH 7.4) plus 2% bovine serum albumin (BSA) and 0.1% Tween 20, termed PBS-BSA. Culture supernatants, purified monoclonal antibodies, or cattle sera were diluted in PBS-BSA and exposed to the blot at room temperature for 2 h. After three washes in PBS plus 0.1% Tween 20, blots were incubated for 1.5 h in peroxidase-conjugated goat anti-mouse IgG antibody (Pierce) or peroxidase-conjugated goat anti-bovine IgG antibody (Vector Labs) diluted 1:20,000 in PBS-BSA. The blots were again washed three times as described above and developed for chemiluminescence using SuperSignal detection reagents (Pierce).

ELISA procedure. Recombinant proteins were applied as a coating on both PolySorp and MaxiSorp ELISA plates (Nunc Brand, Thermo Fisher Scientific). Based on optimization experiments, the following conditions were chosen. Plates were coated with 20 μg/ml recombinant protein in carbonate buffer and blocked in 0.2% casein and 0.1% Tween 20. Serum samples were diluted 1:100 in 0.2% casein and 0.1% Tween 20. For detection, a mouse anti-bovine IgG-peroxidase conjugate was diluted 1:1,000 in 0.2% casein and 0.1% Tween 20 and the wash buffer was PBS with 0.1% Tween 20. In other experiments, a sheep anti-bovine IgM-peroxidase conjugate was used for detection. After incubation, the plate was washed and tetramethylbenzidine (TMB) substrate was added. The substrate reaction was stopped, and the absorbance was read. ELISAs using the Parachek 2 test kit (Prionics AG, Switzerland) were performed according to the manufacturer's specifications.

Protein arrays. Protein arrays were constructed by spotting *E. coli* expressed recombinant proteins on nitrocellulose and processed as described previously (3). Available lipoproteins, membrane proteins, and hypothetical proteins from *M. avium* subsp. *paratuberculosis* were targeted for inclusion on the array, and the remaining proteins were randomly selected from a collection of 600 recombinant proteins. Image capture and densitometry analysis were performed using a Kodak 40000MM image station (Carestream Molecular Imaging). The Carestream software processed each spot at a predetermined size to yield minimum, maximum, median, and mean gray values. Adjusted spot intensities were calculated from the mean gray value and normalized to the corresponding loading controls (array probed with anti-MBP) to account for any slight variation that might be introduced in array production.

AlphaAssay to determine affinity and specificity of monoclonal antibodies. Quantitative binding assays between truncated NlpC, its homolog (MAP1204c), and 14C5 were conducted by employing a luminescent microbead AlphaScreen technology (7, 13). The principle of this assay relies upon a streptavidin donor bead, which recognizes a biotinylated ligand that binds a second target protein, which itself can be adsorbed to acceptor beads that recognize mouse monoclonal IgG. Using this approach, an equilibrium competition binding assay was established in 96-well-format one-half-area-opaque plates using the AlphaScreen anti-mouse IgG kit purchased from PerkinElmer Life Sciences (Waltham, MA) and carried out according to the following general procedures.

NlpC/14C5 competition assays were carried out in a final reaction

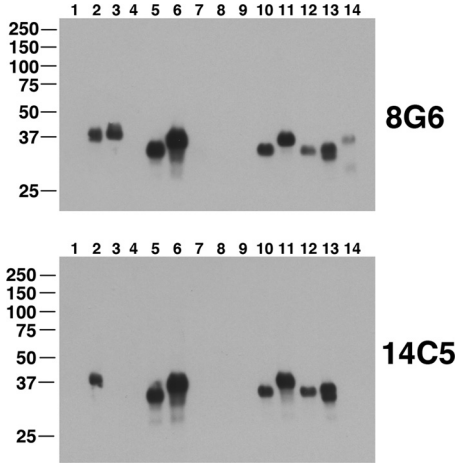

FIG 1 The NlpC/P60 domain-containing protein varies in size among mycobacterial species. Two identical immunoblots were probed with 14C5 and 8G6 as indicated in the right margin. For all lanes, 0.6 μg of the whole-cell lysate was loaded. Lane 1, protein standards; lane 2, *Mycobacterium avium* subsp. *silvaticum*; lane 3, *M. scrofulaceum*; lane 4, *M. abscessus*; lane 5, *M. avium* subsp. *paratuberculosis* K-10; lane 6, *M. avium* subsp. *avium* (ATCC 35713); lane 7, *M. bovis* (ATCC 19210); lane 8, *M. phlei*; lane 9, *M. bovis* BCG; lane 10, *M. avium* subsp. *paratuberculosis* (ATCC 19698); lane 11, *M. avium* subsp. *avium* (ATCC 35716); lane 12, *M. avium* subsp. *paratuberculosis* (ATCC 43015); lane 13, *M. intracellulare*; lane 14, *M. kansasii*. Protein size standards are indicated in kilodaltons in the left margin.

volume of 25 μl by adding each assay component to the following final concentrations: 20 nM biotinylated NlpC-A, 1 nM 14C5, 20 μg/ml anti-mouse IgG AlphaScreen acceptor beads, and 20 μg/ml AlphaScreen streptavidin donor beads. A dilution series for each unlabeled competitor protein was prepared. All reactions were performed in a buffer of PBS (pH 7.4) and 0.1% (vol/vol) Triton X-100. The reaction was performed over the course of 2.5 h and was begun by mixing biotinylated NlpC-A, 14C5, and various concentrations of unlabeled competitor. After 1 h of incubation time at room temperature, this solution was mixed with the acceptor beads and allowed to incubate for an additional hour. Finally, donor beads were added, and after 30 min of incubation time the AlphaScreen signal (photon counts at 630 nm/s) was measured.

The AlphaScreen signal was normalized to wells containing no inhibitor, and a dose-response curve was generated by plotting normalized signal versus log[competitor (M)]. Equilibrium dissociation constants (K_D) were calculated by nonlinear curve fitting to a four-parameter dose-response inhibition curve (variable slope) using GraphPad Prism5 software (GraphPad, La Jolla, CA) as previously described (13).

Statistical analysis. Analysis of reactivity intensities on the protein array included the binomial test in which the null hypothesis *P* value was set to 0.5. Under this null hypothesis, 48 proteins were predicted to show stronger intensity in sera from JD cattle than in sera from healthy cattle and 48 proteins would have a weaker signal in sera from JD cattle than in sera from healthy cattle.

RESULTS

The NlpC protein is larger in non-*paratuberculosis* MAC strains. Two stable hybridomas were obtained after immunizing mice with the full-length NlpC recombinant protein. One hybridoma cell line secreted monoclonal antibody (MAb) 14C5, and the other secreted 8G6. The isotypes for 14C5 and 8G6 are IgG2a and IgG1 heavy chains, respectively. Furthermore, both antibodies are kappa light chain. Immunoblot analysis shows that these antibodies react with both *M. avium* subsp. *paratuberculosis* strains and non-*paratuberculosis* mycobacteria (Fig. 1). Unlike the recently described MAb 17A12, which is 100% specific for *M. avium* subsp. *paratuberculosis* (6), both 8G6 and 14C5 antibodies detected the NlpC protein in MAC strains and *Mycobacterium intracellulare*.

In addition, both 8G6 and 14C5 detected a larger protein in non-*paratuberculosis* mycobacteria than in *M. avium* subsp. *paratuberculosis* (Fig. 1 and 2D). This is contrary to the predicted annotation of each protein. In the *M. avium* subsp. *paratuberculosis* K-10 genome, NlpC is annotated at 316 amino acids (gene identifier [ID], 2720835; calculated size, 33.4 kDa) whereas *Mycobacterium avium* subsp. *hominissuis* strain 104 NlpC is annotated as only a 289-amino-acid protein (gene ID, 4527632; calculated size, 30.2 kDa). Alignment of additional mycobacterial NlpC proteins further suggests that the strain K-10 protein may have been incorrectly annotated. Its 316 annotated residues start with the sequence VRSQ; however, comparison with other annotations of *M. avium* complex strains has suggested that this protein may be only 279 residues long with translation beginning at the methionine of the MKRIY. . . sequence (Fig. 2A). Therefore, in this study, the MKRIY. . . sequence is considered the start of the protein in the K-10 strain and its length is considered to be 279 residues. Table 1 shows the variable lengths of the primary sequence among members of the *Mycobacterium* genus. Amino acid numbers range from 249 in *Mycobacterium tuberculosis* to 311 in *Mycobacterium parascrofulaceum*, with predicted sizes ranging from 26.08 to 32.46 kDa.

The N-terminal half of the protein is highly conserved with only one amino acid difference at position 25 (Pro25Ala) observed between *M. avium* subspecies strains (Fig. 2A). The C-terminal half is more variable, with gaps in the sequence and 12 amino acid differences among the four *M. avium* complex strains examined. The C-terminal half also has a peptide repeat, which likely accounts for the variability in amino acid numbers observed among the different mycobacteria. Note that *M. avium* subsp. *hominissuis* (*M. avium* 104) is the longest polypeptide among these strains. SignalP 3.0 (www.cbs.dtu.dk/services/SignalP-3.0/) predicts an N-terminal signal sequence with a probability of 1.000 and identified a very hydrophobic stretch from residues 3 to 26. The strong potential for a signal sequence influenced the construction of various recombinant expression plasmids described here, such that all three were constructed after the 25th codon (Fig. 2B). In addition, the full-length MAP1272c coding sequence, expressed as a fusion with MBP, was constructed previously (5) and included in these studies. The purity and apparent size of each recombinant protein were evaluated with Coomassie blue-stained SDS-PAGE gels (Fig. 2C).

Monoclonal antibodies 8G6 and 14C5 bind distinct epitopes in NlpC. We also observed different reactivity patterns for each monoclonal antibody (Fig. 1). 8G6 detected *M. scrofulaceum* (lane 3) and weakly recognized *Mycobacterium kansasii* (lane 14), but the 14C5 antibody bound to neither. This suggested distinct epitopes for each antibody, with 8G6 binding to a more conserved epitope. Only *Mycobacterium bovis*, *M. phlei*, and *Mycobacterium abscessus* whole-cell lysates did not react with either antibody. The antibodies were mapped to a specific section of the protein using the truncated peptides described in Fig. 2B and C. These data show that 8G6 reacted with all three peptides whereas 14C5 reacted with only the $A^{(26-279)}$ and $B^{(26-168)}$ truncations (Fig. 3). Therefore, the 14C5 epitope maps to a 49-amino-acid region from positions 26 to 74 on the N-terminal half of the protein whereas 8G6 bound an epitope between amino acids 74 and 168 in the center (compare

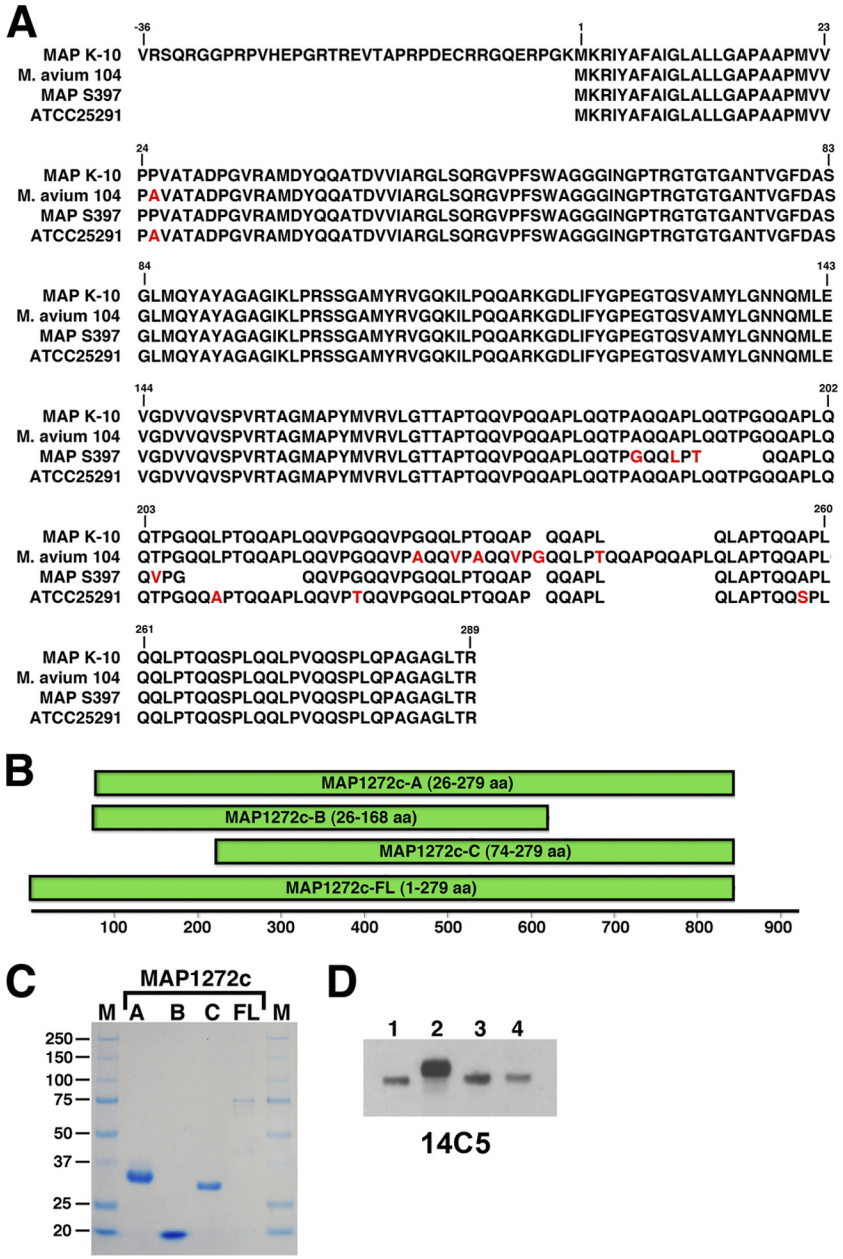

FIG 2 Analysis of recombinant and native NlpC protein. (A) Amino acid sequence alignment of NlpC sequences from four *M. avium* complex strains. Differences are highlighted in red, and gaps are shown. MAP K-10 is a bovine strain of *M. avium* subsp. *paratuberculosis*, MAP S397 is an ovine strain of *M. avium* subsp. *paratuberculosis*, *M. avium* 104 is an *M. avium* subsp. *hominissuis* isolate, and ATCC 25291 is *M. avium* subsp. *avium*. (B and C) The full-length protein and three truncated, overlapping polypeptides are shown schematically on a base pair scale (B) and by SDS-PAGE gel electrophoresis (C). The full-length protein was expressed as a fusion with MBP while the three truncated peptides are polyhistidine tagged (lanes A, B, and C correspond to the A, B, and C peptides in panel B). Lanes M contain protein size markers, and lane FL contains full-length NlpC (amino acids 1 to 279). (D) The native protein is detected by the monoclonal antibody 14C5 from whole-cell extracts of *M. avium* complex strains. Note that *M. avium* subsp. *avium* (ATCC 35713) shows a larger protein than do *M. avium* subsp. *paratuberculosis* strains. Lanes: 1, *M. avium* subsp. *paratuberculosis* K-10; 2, *M. avium* subsp. *avium* (ATCC 35713); 3, *M. avium* subsp. *paratuberculosis* (ATCC 19698); 4, *M. avium* subsp. *paratuberculosis* (ATCC 43015).

Fig. 2B with Fig. 3). Both MAb epitopes appear to be linear, not conformational, as judged by reactivity to denatured antigens following PAGE separation. Although the precise epitopes for each MAb were not defined at a high resolution, these data confirm that 8G6 and 14C5 recognize distinct epitopes.

Characterization of MAb binding to NlpC. More detailed insight into NlpC recognition by 14C5 and 8G6 was also achieved through the use of a no-wash, solution-based binding assay (7). In this approach, termed AlphaAssay, a biotinylated target protein (in this case, NlpC-A) is incubated with a cognate MAb, and the interaction between these two proteins brings a streptavidin-coated luminescent donor bead into physical proximity to an anti-IgG-derivatized luminescent acceptor bead. Biochemical constants, in particular K_d (dissociation constant) values, can then be

TABLE 1 Predicted sizes of NlpC/P60 domain-containing proteins among *Mycobacterium* sequences in the NCBI database

Mycobacterial species/strain(s)	No. of amino acids	Calculated size (kDa)	Accession no.	E value[a]
M. avium subsp. *paratuberculosis* K-10	279	29.22	NP_960206.1	0.0
M avium subsp. *avium* ATCC 25291	279	29.21	ZP_05217173.1	0.0
M. avium subsp. *hominissuis* 104	289	30.24	YP_882390.1	3e−174
M. avium subsp. *paratuberculosis* S397	264	27.61	EGO36914.1	3e−159
M. intracellulare ATCC 13950	293	30.69	ZP_05225218.1	6e−148
M. colombiense CECT 3035	258	27.32	ZP_08717501.1	1e−122
M. kansasii ATCC 12478	277	28.92	ZP_04746612.1	1e−121
M. ulcerans Agy99	259	27.41	YP_905539.1	7e−117
M. marinum M	259	27.41	YP_001850685.1	7e−117
M. parascrofulaceum ATCC BAA-614	311	32.46	ZP_06847019.1	8e−108
M. bovis AF2122/97	230	23.96	NP_855245.1	2e−103
M. tuberculosis H37Rv	230	23.96	NP_216082.1	2e−103
M. tuberculosis CDC1551, F11, KZN 1435	249	26.08	NP_336070.1	2e−103

[a] Database queried with the translated MAP1272c sequence from K-10.

derived by competition of this interaction by including various concentrations of unlabeled proteins in the assay. Interestingly, while a strong signal was generated when biotinylated NlpC-A was captured by 14C5 in this assay, no signal was detected when 8G6 was used as the capturing antibody (data not shown). Since both of these MAbs recognize NlpC-A in the context of an immunoblot (Fig. 3 above), this result strongly suggests that the 8G6 epitope is not surface exposed in soluble NlpC-A.

Further information regarding the interactions between 14C5 and the two epitope-harboring NlpC truncations shown in Fig. 3 was derived from competition binding studies (Fig. 4 and Table 2). This revealed that NlpC-A and NlpC-B bound 14C5 with experimental K_d values of 15.2 and 10.7 nM, respectively. It is noteworthy that the derived 95% confidence intervals for these values overlap one another, which indicates that any differences in 14C5 binding to the NlpC truncations are statistically insignificant. Still, the high affinity of 14C5 for a soluble form of its NlpC antigen suggests that this MAb may be useful as a tool for detecting NlpC in biological samples.

Observations using MAbs in diagnostic tests have demonstrated the possibility that they may cross-react with proteins from closely related species, but they may also react with closely related proteins from the same organism. Indeed, NlpC has four homologs which appear to share the widely distributed NlpC/P60 catalytic domain that is characteristic of NlpC itself. These proteins, encoded by MAP1203, MAP1204, MAP1928c, and MAP0036, share sequence identities of 57, 55, 30, and 35%, respectively, with NlpC encoded by MAP1272c across the region defined by the NlpC/P60 domain (data not shown). Since this level of sequence identity suggested that related NlpC/P60 proteins have the potential to cross-react with 14C5, the ability of this MAb to bind to purified, recombinant MAP1204 was examined (Fig. 4 and Table 2). These results demonstrated that 14C5 had a nearly 1,000-fold-greater affinity for both NlpC fragments expressed from MAP1272c than for that from MAP1204. Thus, this significant affinity change indicates that 14C5 is highly specific for NlpC, even compared to closely related *M. avium* subsp. *paratuberculosis* proteins.

Immunogenicity of the NlpC/P60 protein. The NlpC protein was spotted on a protein array along with 95 other recombinant proteins and analyzed with positive and negative JD serum samples from cattle. A complete listing of the proteins present on the array along with their characteristics appears in Table S4 in the supplemental material. Of these proteins, NlpC consistently

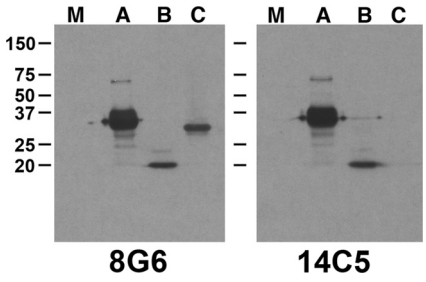

FIG 3 8G6 and 14C5 MAbs bind distinct epitopes in NlpC. Shown are two immunoblots exposed to the antibody indicated. 8G6 detects all three His-tagged proteins whereas 14C5 detects only the proteins in lanes A and B. Lane assignment designations are the same as those in Fig. 2C. The positions of the kilodalton size standards are indicated in the left margins.

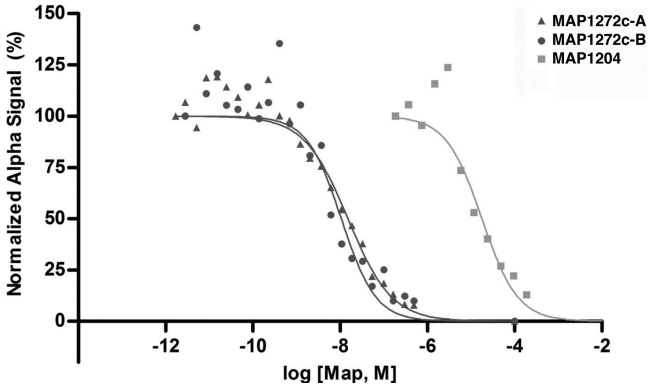

FIG 4 14C5 binds NlpC with low-nanomolar affinity and is highly selective for NlpC versus a closely related protein. A no-wash, solution-based ELISA method was used to determine dissociation constants (K_d) of 14C5 binding to two forms of NlpC as well as that of the homologous protein, MAP1204. Biotinylated MAP1272c-A was incubated with 14C5, and this interaction was competed under equilibrium conditions with a dilution series of various unlabeled proteins. Apparent K_d for each interaction pair were derived from 50% inhibitory concentration values obtained from four-parameter dose-response curves as shown. Whereas the K_d values for 14C5 binding to the MAP1272c A and B fragments are largely identical (15.2 versus 10.7 nM, respectively), the homologous protein, MAP1204, which is 55% identical to MAP1272c, is recognized nearly 1,000-fold more weakly (Table 2).

TABLE 2 14C5 antibody binding constants for selected *M. avium* subsp. *paratuberculosis* proteins

Competitor	K_d[a]	R^2	95% confidence interval (K_D)	No. of points analyzed	No. of outliers	S/N[b]
Map1272cA	15.2 nM	0.957	10.7 to 21.6 nM	25	0	144
Map1272cB	10.7 nM	0.888	6.1 to 18.8 nM	24	0	92
Map1204	17.9 μM	0.958	11.8 to 27.3 μM	11	1	107

[a] K_d is the equilibrium dissociation constant. The smaller the dissociation constant, the tighter the antigen-antibody binding. Parameters for data analysis and curve fitting are found in Materials and Methods.

[b] S/N denotes the ratio of experimental luminescence signal to noise. Background noise levels were obtained by measuring the signal of a mock assay where biotinylated Map1272cA was omitted.

ranked among the most antigenic to positive serum samples (Fig. 5). The positive serum samples (cows 28, 34, 70, and 192) are readily distinguished from the negative serum sample (cow 2) by reactivity with the whole-cell sonicate antigen (spot H12 in Fig. 5). Densitometry analysis was performed on arrays to quantify reactivity levels at each spot. Among the 14 positive JD samples, densitometry analysis shows that NlpC had the strongest reactivity among the recombinant proteins spotted on the array, but not stronger than the whole-cell sonicate (Fig. 6). Cow 2, shown in Fig. 5, had the highest background reactivity among the three negative serum samples but was still well below the positive-sample signals (average intensity of positive samples was 61.2 compared to 9.8 for negative samples in Fig. 6).

The NlpC recombinant protein was next tested along with 9 other proteins ranked among the most immunogenic, yet with the least background reactivity as determined by a previous protein array study (3). These included proteins encoded by MAP0857c, MAP0865, MAP0900, MAP2077c, MAP2116c, MAP3155c, MAP3735c, MAP3817c, and MAP4014. Each served as the coating antigen in an ELISA similar to the

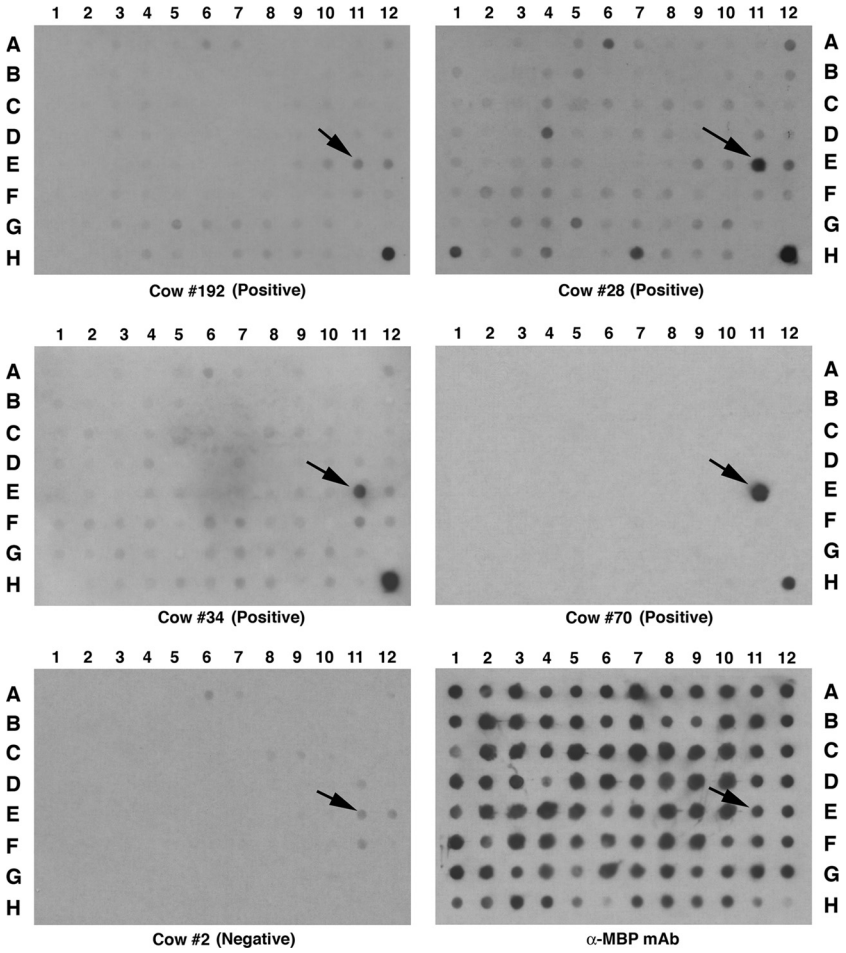

FIG 5 Assessment of the bovine humoral immune response to *M. avium* subsp. *paratuberculosis* recombinant proteins using 96-spot protein arrays. Shown are 6 protein arrays exposed to primary sera as indicated beneath each array. The arrows point to the spot containing the NlpC recombinant protein. The whole-cell sonicate was spotted in H12 (lower right corner in each array). The anti-MBP monoclonal antibody reacts with all proteins on the array and serves as a control to demonstrate the amount of protein spotted. Spot assignments along with densitometry data for each array are present in Tables S4 and S5 in the supplemental material.

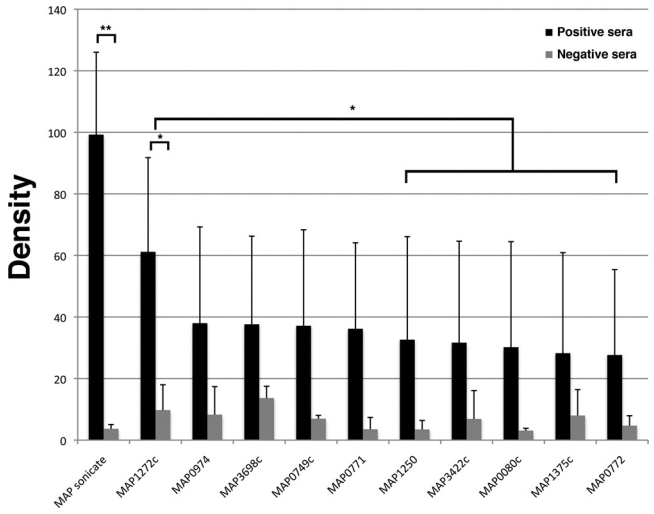

FIG 6 Quantitative densitometry of the most immunogenic arrayed proteins. The density value is a measure of signal intensity for each protein on the array. Reactivity levels were normalized to intensities obtained on the anti-MBP array. Data are assembled from 14 positive sera and 3 negative sera. The average density for NlpC (MAP1272c) was above 60, whereas the average densities for the remaining recombinant proteins were all below 40. Error bars indicate the standard deviations of the means. Significance was determined using a Student unpaired *t* test. *, $P < 0.05$; **, $P < 0.01$.

Parachek ELISA against four positive and four negative JD serum samples (Fig. 7). All of the proteins tested showed strong reactivity to positive sample 4. Reactivity with this sample was due to the presence of anti-MBP antibodies, as demonstrated by preincubation of serum samples with different concentrations of MBP (data not shown). However, NlpC still appeared to be the most promising of the 10 proteins assayed. In order to remove background reactivity associated with the MBP tag, truncated polyhistidine-tagged proteins, with the 6×His tag proteolytically removed, were analyzed to determine which section of NlpC is most immunogenic. The recombinant representing amino acids 74 to 279 (MAP1272c-C) was the most immunoreactive section of the protein (Fig. 8). As a consequence, this fragment was used in subsequent ELISAs.

Comparison of MAP1272c with a commercial ELISA. Because NlpC was the strongest antigen among more than 100 recombinant proteins tested, it was of interest to determine if this antigen might perform better than a commercial ELISA in identifying cattle with Johne's disease. When the MAP1272c-C fragment was tested against different amounts of sera by ELISA, JD positive serum samples (Pos 1 to 3 and 6 to 9) gave high signals when 5 or 10 μl of serum was used (Fig. 9A). Samples Pos 4 and Pos 10 each showed signal increases with the concomitant increase in serum volume added. However, JD positive samples 5, 11, and 12 gave signals at or below the background level observed with the negative serum. Thus, when using 5 μl of serum and 0.5 as the cutoff, the MAP1272c-C fragment detected 9 of the 12 positive samples (75%) and 1 of the 4 negative samples. However, the Parachek 2 ELISA correctly identified all 12 positive samples and did not react with any of the negative samples (data not shown). This indicates that the commercial test was more sensitive than the recombinant antigen alone.

We concluded the study by examining the reproducibility of the MAP1272c ELISA using three independent MAP1272c-C protein preparations on two separate days. The reproducibility is very good in terms of both batch-to-batch consistency and repeatability on different days (Fig. 9B and C). The coefficient of variation (CV) over all variables is less than 10%. For some negative samples, the variation is higher because values are below the linear range. However, even those CVs are below 20%.

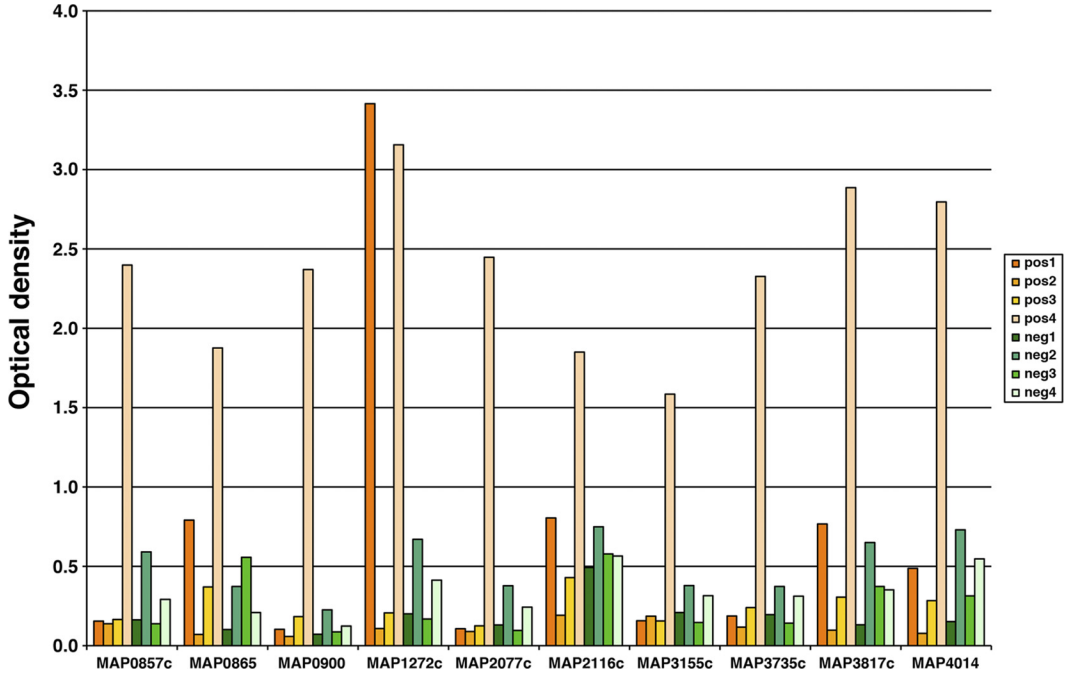

FIG 7 Serum reactivity against candidate antigens of *M. avium* subsp. *paratuberculosis*. Ten recombinant proteins were analyzed by ELISA with four positive and four negative bovine serum samples.

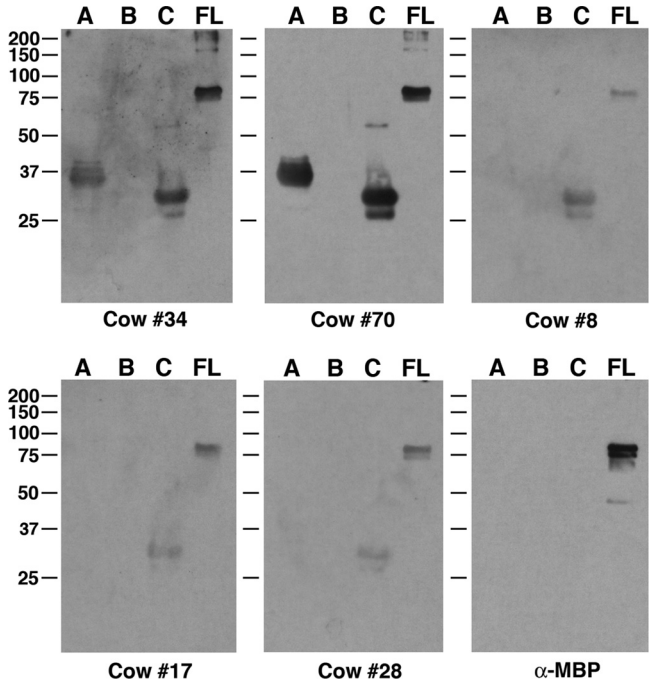

FIG 8 Immunoblot analysis of NlpC peptides with sera from cattle with JD. The serum sample used is indicated beneath each blot. The anti-MBP monoclonal antibody identifies only the MBP fusion protein. Data show that the section from amino acids 74 to 279 is the most immunogenic. Lanes: A, MAP1272c A peptide (amino acids 26 to 279); B, MAP1272c B peptide (amino acids 26 to 168); C, MAP1272c C peptide (amino acids 74 to 279); FL, MAP1272c full-length peptide (amino acids 1 to 279). The positions of the kilodalton size standards are indicated in the left margins.

DISCUSSION

An antibody specific for *M. avium* subsp. *paratuberculosis* was recently discovered by immunizing mice with a surface extract of the bacterium (6). While the antigen that binds to this specific antibody is present in other mycobacteria, it serendipitously binds an epitope containing a single nucleotide polymorphism present only in *M. avium* subsp. *paratuberculosis*. In the present study, NlpC encoded by MAP1272c is also not specific to *M. avium* subsp. *paratuberculosis*, as shown in the sequence alignment in Fig. 2. However, it can be concluded that the 14C5 antibody is specific for MAC strains, comprising *M. intracellulare* and three subspecies of *M. avium* (16, 33). Furthermore, the antibody 8G6 also weakly bound NlpC in *M. kansasii* and *M. scrofulaceum*, two species outside the MAC, and provides evidence that shared determinants exist between these species and members of the MAC group. The lack of antibody binding to *M. bovis* may be surprising given the high similarity of NlpC/P60 domain-containing proteins in Table 1; however, this has been observed with other MAbs generated against *M. avium* subsp. *paratuberculosis* proteins (4) and there are 54 amino acid differences between these species for NlpC. Both of these antibodies demonstrated the variable size of the NlpC protein as expressed from mycobacterial species. This was also suggested based on calculated molecular weights of selected mycobacterial species. The reason for this size difference was not conclusively determined, but sequence analysis suggests that the repeat region of the protein may account for this as observed for other proteins (10).

While it appears that the MAbs described here are not monospecific to *M. avium* subsp. *paratuberculosis*, important features of their reactivity to NlpC identified here may still have importance in efforts toward a more accurate diagnosis of JD. First, while both 8G6 and 14C5 bind to NlpC, only 14C5 is capable of recognizing native, soluble NlpC antigen. Second, the AlphaAssay results demonstrate that 14C5 binds its NlpC target with a low-nanomolar dissociation constant consistent with highly specific protein-protein interactions (Table 2). In addition to this, 14C5 displays high selectivity for NlpC relative to closely related protein antigens, as judged by a roughly 1,000-fold increase in the equilibrium dissociation constant for binding MAP1204 relative to NlpC (Table 2). Separately, examination of the humoral reactivity of JD-positive cattle toward full-length NlpC and its truncations demonstrated that only NlpC-C peptide consistently retained antigenicity comparable to that of the full-length counterpart for most JD-positive cattle. Since this region of NlpC is not recognized by 14C5, it is possible that the complementary desirable features of strong seroreactivity of JD-positive cattle to the NlpC C-terminal region, along with high-affinity binding between 14C5 and NlpC N-terminal regions, could be combined into a sandwich-type immunodiagnostic tool. While additional work is clearly needed in this area, the results presented here constitute a promising starting point for future research and development.

Surface-exposed proteins are best positioned to be major contributors of host cell invasion, and antibodies against such proteins have been shown to be effective at blocking invasion (26, 28). NlpC contains invasion-associated domains in addition to the P60 domain mentioned in the introduction. Furthermore, signal peptide predictions show a 29-amino-acid signal peptide and PSORTb analysis predicts that NlpC is present in the cytoplasmic membrane. Collectively, these results suggest that NlpC may be an invasion protein. Further studies will be performed to determine if either 8G6 or 14C5 antibodies block invasion of intestinal epithelial cells.

Immunodiagnostic techniques may use different types of antigens: whole inactivated cells, lipid, synthetic peptides, or recombinant proteins. The difficulty is finding the best compromise between diagnostic sensitivity and specificity. Immunoblotting allows the simultaneous detection of antibodies with different specificities and the potential detection of different immunological profiles. We investigated the use of truncated NlpC proteins as a potential antigen in the serodiagnosis of JD. MAP1272c was initially shown to encode an antigenic protein when a cell-free transcription-translation system for protein expression was examined (22). The protein produced in that study showed reactivity to positive pooled serum but not to negative pooled serum. However, the *in vitro* expression system yielded low quantities of protein and thus was good only as an initial screening tool.

In order to extend those initial findings, the immunogenicity of the NlpC recombinant protein was tested against over 100 other *M. avium* subsp *paratuberculosis* recombinant proteins using confirmed positive and negative serum samples in this study. While NlpC was the strongest antigen, it was shown that the MBP fusion protein tag resulted in high background with some bovine serum samples due to antibodies against MBP. Using the tag-free versions of the protein eliminated this issue, and it was used as the coating antigen in subsequent ELISAs. ELISAs with this recombinant protein were able to discriminate between most positive and

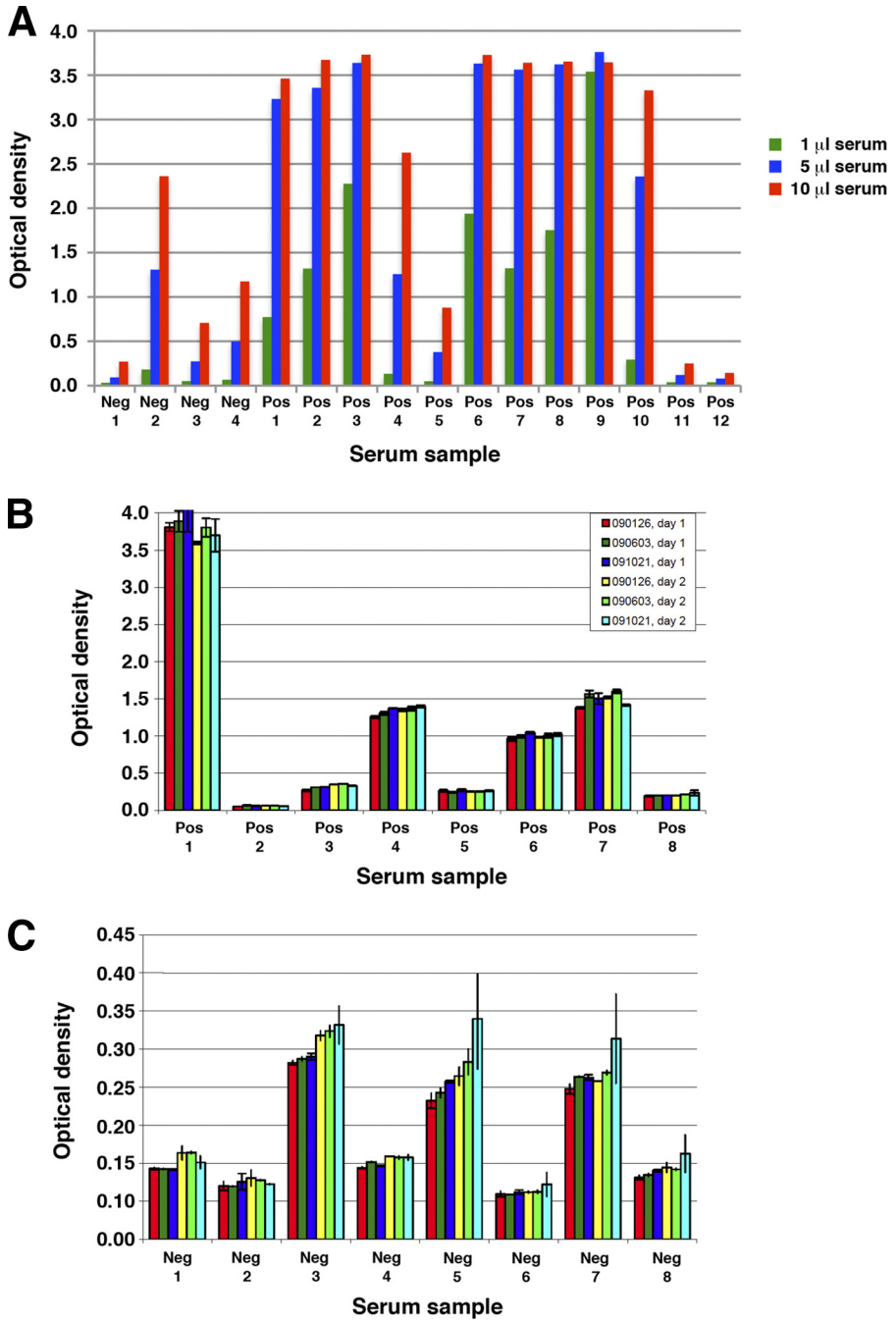

FIG 9 Performance of a MAP1272c-C ELISA. (A) The influence of three different serum amounts for each positive and negative sample is shown. (B and C) The reproducibility among different preparations of the same antigen demonstrates lot-to-lot consistency for both positive (B) and negative (C) serum samples.

negative serum samples, but they did not detect three known positive samples that the Parachek 2 ELISA correctly identified. Thus, even though antigen production was demonstrated to be highly reproducible, it is not more sensitive than the Parachek 2 ELISA at detecting positive serum samples. Furthermore, the NlpC protein reacted strongly to negative serum sample 2 in a dose-dependent manner (Fig. 9). This animal was confirmed negative for Johne's disease but may have been exposed to closely related environmental mycobacteria such as *Mycobacterium avium* subsp. *avium*. If true, this result would highlight the potential for false-positive reactions that can occur when antigens are not specific.

Another recently published study examined two recombinant proteins, encoded by MAP1152 and MAP1156, in comparison to the commercially available Idexx ELISA (2). Those proteins were found to be discriminatory between positive and negative serum samples, but the positive serum reacted more strongly in the Idexx test. Collectively, both that study and the current study demonstrate that recombinant proteins tested thus far do not improve

upon commercially available ELISAs. However, there are many more candidates remaining to be tested, and in all cases, they must be measured against commercially available tests, which serve as the standard that they must surpass (12).

ACKNOWLEDGMENTS

The technical assistance of Janis Hansen (NADC) and Daniel Zwald (Prionics AG) is gratefully acknowledged.

Mention of trade names or commercial products in this article is solely for the purpose of completing research objectives and does not imply recommendation or endorsement by the U.S. Department of Agriculture.

This work was funded in part by a grant to B.V.G. from the Missouri Life Sciences Research Board (13238-2007).

REFERENCES

1. **Aramini JM, et al.** 2008. Solution NMR structure of the NlpC/P60 domain of lipoprotein Spr from *Escherichia coli*: structural evidence for a novel cysteine peptidase catalytic triad. Biochemistry **47**:9715–9717.
2. **Bannantine JP, et al.** 2011. Immunogenicity and reactivity of novel *Mycobacterium avium* subsp. *paratuberculosis* PPE MAP1152 and conserved MAP1156 proteins with sera from experimentally and naturally infected animals. Clin. Vaccine Immunol. **18**:105–112.
3. **Bannantine JP, et al.** 2008. Profiling bovine antibody responses to *Mycobacterium avium subsp. paratuberculosis* infection by using protein arrays. Infect. Immun. **76**:739–749.
4. **Bannantine JP, et al.** 2007. Production and characterization of monoclonal antibodies against a major membrane protein of *Mycobacterium avium* subsp. *paratuberculosis.* Clin. Vaccine Immunol. **14**:312–317.
5. **Bannantine JP, Stabel JR, Bayles DO, Geisbrecht BV.** 2010. Characteristics of an extensive *Mycobacterium avium* subspecies *paratuberculosis* recombinant protein set. Protein Expr. Purif. **72**:223–233.
6. **Bannantine JP, Stabel JR, Lamont EA, Briggs RE, Sreevatsan S.** 2011. Monoclonal antibodies bind a SNP-sensitive epitope that is present uniquely in *Mycobacterium avium* subspecies *paratuberculosis.* Front. Microbiol. **2**:163. doi:10.3389/fmicb.2011.00163.
7. **Bielefeld-Sevigny M.** 2009. AlphaLISA immunoassay platform—the "no-wash" high-throughput alternative to ELISA. Assay Drug Dev. Technol. **7**:90–92.
8. **Braunstein M, Espinosa BJ, Chan J, Belisle JT, Jacobs WR, Jr.** 2003. SecA2 functions in the secretion of superoxide dismutase A and in the virulence of *Mycobacterium tuberculosis.* Mol. Microbiol. **48**:453–464.
9. **Chen JW, et al.** 2012. Immunogenicity and protective efficacy of the *Mycobacterium avium subsp. paratuberculosis* attenuated mutants against challenge in a mouse model. Vaccine **30**:3015–3025.
10. **Denison AM, Clapper B, Dybvig K.** 2005. Avoidance of the host immune system through phase variation in *Mycoplasma pulmonis.* Infect. Immun. **73**:2033–2039.
11. **Dennis MM, et al.** 2008. Association of severity of enteric granulomatous inflammation with disseminated *Mycobacterium avium* subspecies *paratuberculosis* infection and antemortem test results for paratuberculosis in dairy cows. Vet. Microbiol. **131**:154–163.
12. **Fry MP, Kruze J, Collins MT.** 2008. Evaluation of four commercial enzyme-linked immunosorbent assays for the diagnosis of bovine paratuberculosis in Chilean dairy herds. J. Vet. Diagn. Invest. **20**:329–332.
13. **Garcia BL, et al.** 2012. Diversity in the C3b contact residues and tertiary structures of the staphylococcal complement inhibitor (SCIN) protein family. J. Biol. Chem. **287**:628–640.
14. **Geisbrecht BV, Bouyain S, Pop M.** 2006. An optimized system for the expression and purification of secreted bacterial proteins. Protein Expr. Purif. **46**:23–32.
15. **Harlow E, Lane D (ed).** 1988. Antibodies: a laboratory manual, 1st ed. Cold Spring Harbor Laboratory Press, Cold Spring Harbor, NY.
16. **Inderlied CB, Kemper CA, Bermudez LE.** 1993. The *Mycobacterium avium* complex. Clin. Microbiol. Rev. **6**:266–310.
17. **Kawaji S, Gumber S, Whittington RJ.** 2012. Evaluation of the immunogenicity of *Mycobacterium avium* subsp. *paratuberculosis* (MAP) stress-associated recombinant proteins. Vet. Microbiol. **155**:298–309.
18. **Lenz LL, Mohammadi S, Geissler A, Portnoy DA.** 2003. SecA2-dependent secretion of autolytic enzymes promotes *Listeria monocytogenes* pathogenesis. Proc. Natl. Acad. Sci. U. S. A. **100**:12432–12437.
19. **Lenz LL, Portnoy DA.** 2002. Identification of a second *Listeria secA* gene associated with protein secretion and the rough phenotype. Mol. Microbiol. **45**:1043–1056.
20. **Leroy B, et al.** 2009. Use of *Mycobacterium avium subsp. paratuberculosis* specific coding sequences for serodiagnosis of bovine paratuberculosis-.Vet. Microbiol. **135**:313–319.
21. **Li L, et al.** 2005. The complete genome sequence of *Mycobacterium avium* subspecies *paratuberculosis.* Proc. Natl. Acad. Sci. U. S. A. **102**:12344–12349.
22. **Li L, et al.** 2007. Rapid expression of *Mycobacterium avium* subsp. *paratuberculosis* recombinant proteins for antigen discovery. Clin. Vaccine Immunol. **14**:102–105.
23. **Mikkelsen H, Aagaard C, Nielsen SS, Jungersen G.** 2011. Review of *Mycobacterium avium subsp. paratuberculosis* antigen candidates with diagnostic potential.Vet. Microbiol. **152**:1–20.
24. **Milner AR, Lepper AW, Symonds WN, Gruner E.** 1987. Analysis by ELISA and Western blotting of antibody reactivities in cattle infected with *Mycobacterium paratuberculosis* after absorption of serum with *M phlei.* Res. Vet. Sci. **42**:140–144.
25. **Nielsen SS, Toft N.** 2008. Ante mortem diagnosis of paratuberculosis: a review of accuracies of ELISA, interferon-gamma assay and faecal culture techniques. Vet. Microbiol. **129**:217–235.
26. **Pentecost M, Otto G, Theriot JA, Amieva MR.** 2006. *Listeria monocytogenes* invades the epithelial junctions at sites of cell extrusion. PLoS Pathog. **2**:e3. doi:10.1371/journal.ppat.0020003.
27. **Raizman EA, Fetrow JP, Wells SJ.** 2009. Loss of income from cows shedding *Mycobacterium avium* subspecies *paratuberculosis* prior to calving compared with cows not shedding the organism on two Minnesota dairy farms. J. Dairy Sci. **92**:4929–4936.
28. **Rezcallah MS, et al.** 2005. Engagement of CD46 and alpha5beta1 integrin by group A streptococci is required for efficient invasion of epithelial cells. Cell. Microbiol. **7**:645–653.
29. Reference deleted.
30. **Stabel JR.** 2008. Pasteurization of colostrum reduces the incidence of paratuberculosis in neonatal dairy calves. J. Dairy Sci. **91**:3600–3606.
31. **Sugden EA, Samagh BS, Bundle DR, Duncan JR.** 1987. Lipoarabinomannan and lipid-free arabinomannan antigens of *Mycobacterium paratuberculosis.* Infect. Immun. **55**:762–770.
32. **Sullivan JT, Young EF, McCann JR, Braunstein M.** 2012. The *Mycobacterium tuberculosis* SecA2 system subverts phagosome maturation to promote growth in macrophages. Infect. Immun. **80**:996–1006.
33. **Thorel MF, Krichevsky M, Levy-Frebault VV.** 1990. Numerical taxonomy of mycobactin-dependent mycobacteria, emended description of Mycobacterium avium, and description of *Mycobacterium avium* subsp. *avium* subsp. nov., *Mycobacterium avium* subsp. *paratuberculosis* subsp. nov., and *Mycobacterium avium* subsp. *silvaticum* subsp. nov. Int. J. Syst. Bacteriol. **40**:254–260.
34. **Tsuge Y, Ogino H, Teramoto H, Inui M, Yukawa H.** 2008. Deletion of cgR_1596 and cgR_2070, encoding NlpC/P60 proteins, causes a defect in cell separation in *Corynebacterium glutamicum* R. J. Bacteriol. **190**:8204–8214.
35. **Waters WR, et al.** 2003. Early induction of humoral and cellular immune responses during experimental *Mycobacterium avium* subsp. *paratuberculosis* infection of calves. Infect. Immun. **71**:5130–5138.
36. Reference deleted.
37. Reference deleted.
38. **Yokomizo Y, Merkal RS, Lyle PA.** 1983. Enzyme-linked immunosorbent assay for detection of bovine immunoglobulin G1 antibody to a protoplasmic antigen of *Mycobacterium paratuberculosis.* Am. J. Vet. Res. **44**:2205–2207.
39. **Yokomizo Y, Yugi H, Merkal RS.** 1985. A method for avoiding false-positive reactions in an enzyme-linked immunosorbent assay (ELISA) for the diagnosis of bovine paratuberculosis. Nippon Juigaku Zasshi **47**:111–119.